Magnetic Resonance Imaging and Histological Analysis of Beta-Amyloid Plaques in Both Human Alzheimer's Disease and APP/PS1 Transgenic Mice

M. D. Meadowcroft[1,2], J. R. Connor[3], M. B. Smith[1], and Q. X. Yang[1,3]

[1]Radiology, Pennsylvania State University - College of Medicine, Hershey, PA, United States, [2]Neural and Behavioral Sciences, Pennsylvania State University - College of Medicine, Hershey, PA, United States, [3]Neurosurgery, Pennsylvania State University - College of Medicine, Hershey, PA, United States

Introduction: Imaging of beta amyloid beta-amyloid (Aβ) plaques in human Alzheimer 's disease (AD) and the APP/PS1 mouse model has been of great interest for AD research. However, the histo-pathological basis of the image contrast associated with Aβ plaques and the connected relaxation mechanism has not been well-understood. With the aid of the previously developed histological coil, T_2*-weighted images and R_2* parametric maps were directly compared to histology stains acquired from the same set of Alzheimer's and APP/PS1 tissue slices. The goal of the current study is to use this novel technology to a) establish the relationship between MR image contrast associated with Aβ plaques and their histology and b) compare such relationships in human and transgenic APP/PS1 mouse tissues. Examination of the relationship between MR contrast due to beta-amyloid plaque morphology and iron deposition both in human AD and the APP/PS1 model is described.

Methods: Entorhinal cortex brain tissue samples from clinically and histologically determined AD subjects (n=5) and age-matched controls (n=4) as well as tissue from transgenic mice (n=5) inserted with chimeric amyloid precursor protein (APP) and a mutant human presenilin 1 and age matched cage mate C57BL/6 control mice (n=3) were used. Tissue sections were cut at 60μm and prepared for MR micro-imaging using a 7.0 T magnet with the histological coil (1). A T_2* MGE sequence was utilized with a matrix of 512^2 and a final pixel resolution of 45μm x 45μm in the through – plane direction. After histological MR imaging, the 60μm tissue sections were co-stained with Thioflavin-S for Aβ plaque detection and both a traditional and modified Perl's stain to stain for ferric iron. Samples were also prepared for transmission electron microscopy for high magnification histological imaging of plaques. R_2* parameter maps were created and detailed relaxation measurements of individual plaques in both human AD and APP/PS1 tissue were evaluated.

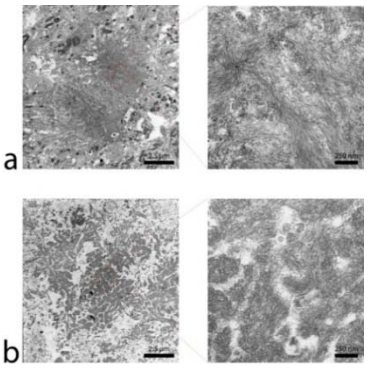

Figure 2: Transmission electron microscope images of plaques in (a) APP/PS1 and (b) human AD tissue (6000x left, 46000x of selected region right). The denser of the beta-amyloid plaques in the APP/PS1 compared to the human AD tissue is illustrated along with the increased amount gaps between amyloid strand clusters in the human AD tissue compared to the APP/PS1 tissue.

Results: Figure 1 (left) shows a T_2* weighted MR image and histological images co-stained with thioflavin-S for beta-amyloid plaques and a traditional Perl's stain for ferric iron (Fe^{+3}) within the same tissue section from the entorhinal cortex of an AD subject. Many dark spots can clearly be observed in the gray matter in the MR image. Those hypo-intensities in the MR images correspond to either punctate green fluorescent thioflavin-S positive Aβ-plaques (red arrows) or dark brown patches indicating regions of high focal iron such as hemosiderin or magnetite deposits (blue arrows). The widespread dark spots seen in the human tissue are also shown conspicuously in the T_2* image of the transgenic animal tissue within the piriform cortex (Fig 1, right). No dark iron cored plaques were observed in the transgenic animal histological images compared to the human AD sections. Transgenic animal tissue shows a high concentration of large amyloid deposits while co-staining with the traditional Perl's ferric iron stain does not show regions of high iron within the these plaques. There is visible evidence of trace amounts of iron in the transgenic animal plaques that was not stainable with the traditional method, while very minute compared to the human AD tissue. Differences between human AD and the APP/PS1 Aβ plaques are most noticeable in the TEM magnifications (Fig. 2). The human AD plaques consist of fragmented patches with random fibrillar orientation in the amyloid core while the structure of transgenic mouse plaques appears to be a highly packed aggregation of long and oriented fibrils. The decreased density of the amyloid core creates gaps that are prevalent in the human AD plaques while rarely found in the transgenic mouse plaques. R_2* for human regions with plaques were significantly higher ($p<0.0001$) then both the controls and regions without plaques (Fig. 3a). Regions with plaques in the APP/PS1 animals had a significantly higher R_2* compared to both control tissue and regions without plaques ($p<0.0001$).

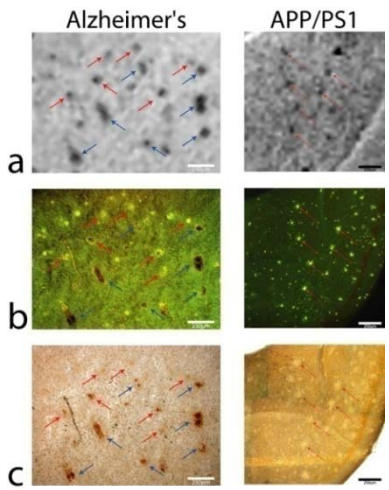

Figure 1: T_2* weighted MR image (a) and histological images of Thioflavin-S stain for beta-amyloid plaques(b) and (c) Perl's iron stain of the same tissue section from the entorhinal cortex of an Alzheimer's disease subject (left) and APP/PS1 mouse (right). The figure illustrates that hypo-intensities seen in the Human AD T_2* weighted image correlate to plaque location and focal iron concentrations. The APP/PS1tissue shows similar hypo-intensities associated with plaques with much reduced iron load.

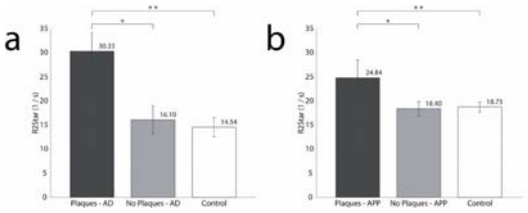

Figure 3: Bar graphs of average R_2* rates from ROI's with plaques, without plaques and control tissue within human (a) and mouse tissue (b). The R_2* relaxation of plaque ROI's in the AD tissue have a significantly higher R_2* than regions without plaques and control tissue sections. A similar trend is found in mouse data.

Discussion: Imaging of thin slices of tissue samples with the aid of the histological coil allows the one-to-one comparison of tissue pathology as seen in histological stains and different MRI methodologies. With this technique, the relaxation mechanisms for Aβ plaques in human Alzheimer's disease and the APP/PS1 mouse model were investigated with respect to their morphology and relationship with iron deposition. Thioflavin-S staining for Aβ plaque detection and a Perl's – DAB stain for iron exposure demonstrate a consistent high iron concentration in and around the plaques in human AD samples. The Aβ plaques in human brain samples coincide with the dark spots seen in MRI T_2*-weighted images demonstrating that elevated iron in and around the Aβ plaques deposits plays a part in generating Aβ plaque MRI contrast. Transgenic APP/PS1 brain samples also demonstrate a similar T_2* – weighted MRI contrast associated with Aβ plaque distribution. However, the corresponding iron and Aβ staining morphology appear to differ from the human AD tissue. The iron concentration in the transgenic Aβ plaques is consistently less than that of the human AD plaques. The mean R_2* time for the selected amyloid plaques in the Alzheimer's tissues (Fig. 3) is on average 90% greater than that from the ROI's without plaques and control tissue, while mean R_2* for the selected amyloid plaques is on average 56% higher than in the ROI's without plaques and in the control tissue. The data suggest that iron load alone does not account for the hypo-intensities that are observed in the T_2*-weighted images of the animal pathology. Faster T_2* relaxation resulting in signal drop could be attributable to the dense fibrillar nature of the amyloid beta deposits. The dense formation of the animal plaques would prohibit free water from accessing the core of the plaque as indicated with the TEM data. Thus, our data suggests a dual relaxation mechanism in the generation of T_2* contrast due to Aβ plaques. The focal iron concentration is the dominant cause for rapid T_2* relaxation in human AD plaques while the increased fibrillar density and compacted morphology becomes a major factor for T_2* shortening in the APP/PS1 transgenic plaques.

References: 1 – Meadowcroft *et al.* Mag. Reson. Med. 2007; 57(5): 835 – 841